UNIVERSITY OF AMSTERDAM

UvA-DARE (Digital Academic Repository)

A New Generation of FRET Sensors for Robust Measurement of Gαi1, Gαi2 and Gαi3 Activation Kinetics in Single Cells

van Unen, J.; Stumpf, A.D.; Schmid, B.; Reinhard, N.R.; Hordijk, P.L.; Hoffmann, C.; Gadella (jr.), T.W.J.; Goedhart, J.

DOI
10.1371/journal.pone.0146789

Publication date
2016

Document Version
Final published version

Published in
PLoS ONE

License
CC BY

Link to publication

Citation for published version (APA):
van Unen, J., Stumpf, A. D., Schmid, B., Reinhard, N. R., Hordijk, P. L., Hoffmann, C., Gadella (jr.), T. W. J., & Goedhart, J. (2016). A New Generation of FRET Sensors for Robust Measurement of $G\alpha_{i1}$, $G\alpha_{i2}$ and $G\alpha_{i3}$ Activation Kinetics in Single Cells. *PLoS ONE*, *11*(1), [e0146789]. https://doi.org/10.1371/journal.pone.0146789

General rights
It is not permitted to download or to forward/distribute the text or part of it without the consent of the author(s) and/or copyright holder(s), other than for strictly personal, individual use, unless the work is under an open content license (like Creative Commons).

Disclaimer/Complaints regulations
If you believe that digital publication of certain material infringes any of your rights or (privacy) interests, please let the Library know, stating your reasons. In case of a legitimate complaint, the Library will make the material inaccessible and/or remove it from the website. Please Ask the Library: https://uba.uva.nl/en/contact, or a letter to: Library of the University of Amsterdam, Secretariat, Singel 425, 1012 WP Amsterdam, The Netherlands. You will be contacted as soon as possible.
UvA-DARE is a service provided by the library of the University of Amsterdam (https://dare.uva.nl)

Download date:26 Jul 2022

PLOS ONE

RESEARCH ARTICLE

A New Generation of FRET Sensors for Robust Measurement of $G\alpha_{i1}$, $G\alpha_{i2}$ and $G\alpha_{i3}$ Activation Kinetics in Single Cells

Jakobus van Unen[1], Anette D. Stumpf[2], Benedikt Schmid[2], Nathalie R. Reinhard[1,3], Peter L. Hordijk[1,3], Carsten Hoffmann[2], Theodorus W. J. Gadella, Jr.[1], Joachim Goedhart[1]*

1 Swammerdam Institute for Life Sciences, Section of Molecular Cytology, van Leeuwenhoek Centre for Advanced Microscopy, University of Amsterdam, P.O. Box 94215, NL-1090 GE, Amsterdam, The Netherlands, **2** Bio-Imaging-Center/Rudolf-Virchow-Zentrum and Department of Pharmacology and Toxicology, University of Wuerzburg, Versbacher Strasse 9, 97078, Wuerzburg, Germany, **3** Department of Molecular Cell Biology, Sanquin Research and Landsteiner Laboratory, Academic Medical Center, University of Amsterdam, NL-1066 CX, Amsterdam, the Netherlands

* j.goedhart@uva.nl

CrossMark
click for updates

OPEN ACCESS

Citation: van Unen J, Stumpf AD, Schmid B, Reinhard NR, Hordijk PL, Hoffmann C, et al. (2016) A New Generation of FRET Sensors for Robust Measurement of $G\alpha_{i1}$, $G\alpha_{i2}$ and $G\alpha_{i3}$ Activation Kinetics in Single Cells. PLoS ONE 11(1): e0146789. doi:10.1371/journal.pone.0146789

Editor: Mikel Garcia-Marcos, Boston University School of Medicine, UNITED STATES

Received: September 25, 2015

Accepted: December 22, 2015

Published: January 22, 2016

Copyright: © 2016 van Unen et al. This is an open access article distributed under the terms of the Creative Commons Attribution License, which permits unrestricted use, distribution, and reproduction in any medium, provided the original author and source are credited.

Data Availability Statement: All relevant data are within the paper and its Supporting Information files.

Funding: The authors have no support or funding to report.

Competing Interests: The authors have declared that no competing interests exist.

Abstract

G-protein coupled receptors (GPCRs) can activate a heterotrimeric G-protein complex with subsecond kinetics. Genetically encoded biosensors based on Förster resonance energy transfer (FRET) are ideally suited for the study of such fast signaling events in single living cells. Here we report on the construction and characterization of three FRET biosensors for the measurement of $G\alpha_{i1}$, $G\alpha_{i2}$ and $G\alpha_{i3}$ activation. To enable quantitative long-term imaging of FRET biosensors with high dynamic range, fluorescent proteins with enhanced photophysical properties are required. Therefore, we use the currently brightest and most photostable CFP variant, mTurquoise2, as donor fused to $G\alpha_i$ subunit, and cp173Venus fused to the $G\gamma_2$ subunit as acceptor. The $G\alpha_i$ FRET biosensors constructs are expressed together with $G\beta_1$ from a single plasmid, providing preferred relative expression levels with reduced variation in mammalian cells. The $G\alpha_i$ FRET sensors showed a robust response to activation of endogenous or over-expressed alpha-2A-adrenergic receptors, which was inhibited by pertussis toxin. Moreover, we observed activation of the $G\alpha_i$ FRET sensor in single cells upon stimulation of several GPCRs, including the LPA_2, M_3 and BK_2 receptor. Furthermore, we show that the sensors are well suited to extract kinetic parameters from fast measurements in the millisecond time range. This new generation of FRET biosensors for $G\alpha_{i1}$, $G\alpha_{i2}$ and $G\alpha_{i3}$ activation will be valuable for live-cell measurements that probe $G\alpha_i$ activation.

Introduction

The $G\alpha_i$ subclass of heterotrimeric G-proteins consists of 3 members in humans, $G\alpha_{i1,2,3}$ encoded by the genes GNAI1, GNAI2, GNAI3 [1] and is activated by a wide range of G-protein coupled receptors. The $G\alpha_i$ family of G-proteins have been implicated in numerous pathologies, from involvement in obesity and diabetes [2], functions in the immune system [3] to their

critical roles in several stages of cancer biology [4–7]. Activation of $G\alpha_i$ is predominantly linked to the inhibition of adenylate cyclases, which leads to decreased cAMP accumulation in cells. However, activation of $G\alpha_i$ has more recently been connected to several other molecular effectors, including PI3K/Akt [8,9], ERK [10] and c-Src [5].

The measurement of $G\alpha_i$ activation is classically performed by measuring the inhibition of forskolin-induced cAMP production. Similar to phosphorylation assays further downstream, such measurements lack spatial resolution, have limited temporal resolution and can be influenced by considerable crosstalk and amplification or desensitization of the signal [11–13].

To investigate G-protein activation in a direct way with high spatiotemporal resolution, genetically encoded FRET (Förster Resonance Energy Transfer) or BRET (Bioluminescent Resonance Energy Transfer) biosensors can be employed [14]. These methods are based on the measurement of the non-radiative energy transfer from a donor molecule to an acceptor molecule, which only takes place when donor and acceptor are in close proximity of each other (<10nm). Changes in distance or orientation between the donor and acceptor dipole result in changes in the RET efficiency, which can be quantified.

The RET techniques allow for single cell recordings of the kinetics with millisecond resolution, which can be used to identify cell-to-cell heterogeneity and record pharmacokinetic parameters. Moreover, this approach has the potential to record GPCR activation under physiological conditions in vivo [15].

$G\alpha_i$ has been successfully tagged at different internal sites with luciferase and used for BRET measurements between different $G\alpha_i$ subunits and GPCRs [16–19] or Gγ [19]. FRET measurements between fluorescently tagged $G\alpha_{i1}$, $G\alpha_{i2}$ and $G\alpha_{i3}$ and Gβ [20] or Gγ [21] have also been performed.

To perform FRET measurements, a spectrally overlapping donor and acceptor pair is necessary [24], and it was previously shown that the use of brighter fluorescent proteins can improve the sensitivity of FRET biosensor measurements [22,23]. In order to obtain robust FRET measurements that probe $G\alpha_i$ activation, we have made fusions of $G\alpha_{i1}$ $G\alpha_{i2}$ and $G\alpha_{i3}$ with the brightest and most photostable monomeric cyan fluorescent protein (CFP) currently available, mTurquoise2 (mTq2) [25]. As acceptor we have used circular permutated Venus (cpVenus) fused to $G\gamma_2$, which has previously been used as acceptor in a single plasmid $G\alpha_q$ FRET sensor [26]. We use a single plasmid strategy to facilitate transfection protocols and allow a well-defined donor and acceptor expression ratio in cells [27]. This expression strategy should greatly facilitate the use and reproducibility of the results of these sensors. We present the construction strategy, validation and characterization of this new generation of FRET sensors for the activation of $G\alpha_{i1}$ $G\alpha_{i2}$ and $G\alpha_{i3}$. These biosensors are very well suited for live cell microscopy and can be used for fast kinetic measurements in the millisecond range, allowing pharmacological drug characterization and determination of on- and off-kinetics for agonists and antagonists at $G\alpha_i$–coupled GPCRs.

Results

Generation of constructs

The monomeric CFP variant mTurquoise2, the preferred donor in CFP-YFP FRET pairs due to its high quantum yield and photostability [25], was inserted into $G\alpha_{i1}$ after the alanine on position 121 in the αB-αC loop. This insertion site that was previously shown to retain nucleotide exchange and GTPase reaction rates comparable to wild-type protein [20]. $G\alpha_{i1}$-mTq2 displays plasma membrane localization when expressed in HeLa cells (Fig 1A). Trial experiments were performed to examine whether $G\alpha_{i1}$-mTq2 is suitable for measuring, by means of FRET, the activation of the heterotrimeric G-protein complex upon GPCR activation. To this end,

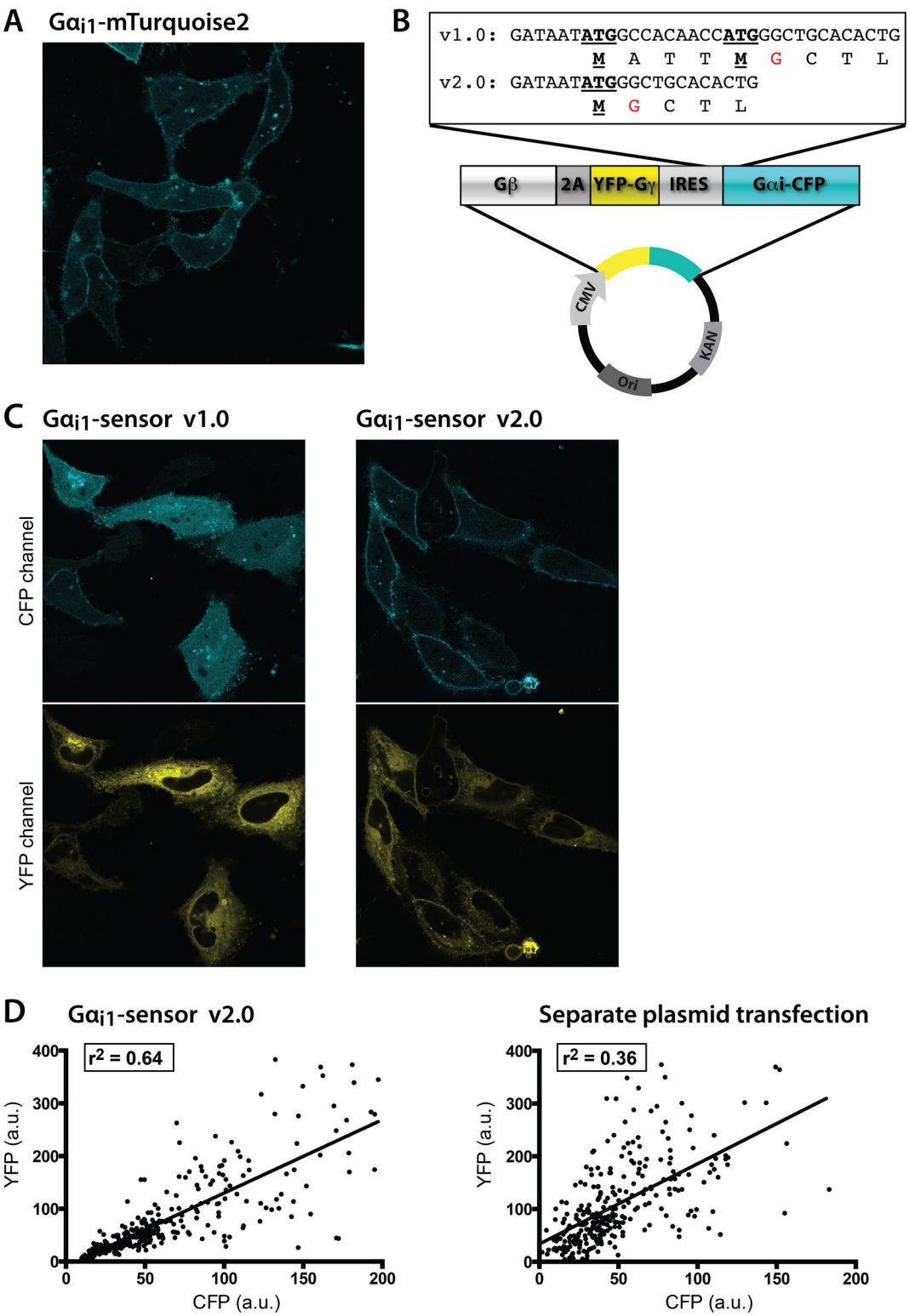

Fig 1. Development and characterization of the new Gα$_{i1}$-sensor. (A) Representative image showing the plasma membrane localization of Gα$_{i1}$ fused to mTurquoise2-Δ9, expressed in HeLa cells. (B) Schematic overview of the plasmid containing pGβ-2A-YFP-Gγ$_2$-IRES-Gα$_{i1}$-CFP, driven by a CMV promoter. The inset shows the DNA sequence encoding the end of the IRES sequence and the start of the Gα$_{i1}$ sequence. The proposed protein translation is shown in the line below the DNA sequence (single letter abbreviations of the amino acids). (C) Confocal images of the localization of Gα$_{i1}$-mTurquoise2-Δ9 (*top row*) and cp173Venus-Gγ$_2$ (*bottom row*) in HeLa cells, for variant 1.0 (*left column*) and variant 2.0 (*right column*) of the Gα$_{i1}$-sensor. (D) Quantitative co-

expression analysis of the CFP and YFP channels of the cp173Venus-$G\gamma_2$ and $G\alpha_{i1}$-mTurquoise2-Δ9 transfections in HeLa cells. Single plasmid transfection (*left*) versus the transfection of the separate plasmids (*right*). The dots depict the CFP and YFP intensity, quantified from individual single cells. The r^2 is the coefficient of determination. Width of the individual images in A and C is 143μm.

doi:10.1371/journal.pone.0146789.g001

both Gβ as well as Gγ can be tagged with an acceptor to measure heterotrimeric G-protein activation by FRET [20,21]. We have previously shown that the highest FRET contrast, for $G\alpha_q$, is obtained with cpVenus-$G\gamma_2$ [26]. Since $G\alpha_i$ has high structural homology to $G\alpha_q$ and the site at which mTurquoise2 is inserted is similar, we decided to employ the same FRET acceptor here. Hence, to introduce a labeled heterotrimeric G-protein complex in cells, we co-expressed $G\alpha_{i1}$-mTq2 together with the FRET acceptor cpVenus-$G\gamma_2$ and untagged $G\beta_1$ [26]. Stimulation of the co-expressed α_2 adrenergic receptor (α_2AR) with UK14,304 shows a rapid increase in CFP fluorescence and a concomitant loss of sensitized emission from the YFP channel, reflecting a loss of FRET. The loss of FRET can be interpreted as a dissociation of the heterotrimer or a change in relative conformation of donor and acceptor. To enable robust co-expression of the different components of the multimeric FRET sensor, we introduced the subunits on the same plasmid, as we reported previously for a $G\alpha_q$ sensor (Fig 1B) [26]. This strategy uses a viral 2A peptide and an IRES sequence to ensure optimal relative levels of the donor ($G\alpha_{i1}$-mTq2) and acceptor (cpVenus-$G\gamma_2$) within single cells, while minimizing cell-to-cell expression heterogeneity in the sample. After generating our first variant, we noticed that $G\alpha_{i1}$-mTq2 was mislocalised in the cytoplasm in many cells (Fig 1C). The $G\alpha_{i1}$ subunit is myristoylated and requires a glycine residue immediately following its starting methionine. Detailed inspection of the plasmid sequence revealed an additional starting codon for the $G\alpha_{i1}$-mTq2 upstream of the native start-codon, generated by the IRES sequence (Fig 1B). We hypothesized that in our first variant of the sensor, most of the $G\alpha_{i1}$-mTq2 protein produced was translated from the upstream methionine in the IRES sequence, which does not result in myristoylated protein. We removed the upstream methionine by whole-vector PCR (see material and methods), which only leaves the native starting codon of $G\alpha_{i1}$-mTq2, followed by a Glycine providing the consensus sequence for myristoylation. Indeed, after transfecting cells with the new plasmid, we observed correctly localized $G\alpha_{i1}$-mTq2 (Fig 1B and 1C). A $G\alpha_{i2}$-sensor and $G\alpha_{i3}$-sensor were constructed in a similar way. To examine the co-expression of the three subunits ($G\alpha_{i1}$-mTq2, $G\beta_1$ and cpVenus-$G\gamma_2$) from a single plasmid versus three separate plasmids, we quantified the CFP and YFP fluorescence in these two experimental conditions (Fig 1D). The CFP and YFP fluorescence in the single plasmid strategy transfection had a coefficient of determination r^2 of 0.64, whereas transfections with the three separate plasmids showed a coefficient of determination r^2 of 0.36 between CFP intensity and YFP intensity. In other words, the correlation between CFP and YFP expression is better in the single plasmid configuration, indicating a clear advantage of this design. An additional advantage of this plasmid is the 3:1 protein expression upstream and downstream of the IRES sequence, which has previously been shown to result in a preferred donor (CFP) and acceptor (YFP) expression ratio for an analogous $G\alpha_q$ FRET sensor [27]. Finally, the single plasmid constructs will simplify introduction into primary cells, the generation of stable cell lines or transgenic organisms with $G\alpha_i$-sensors.

Performance in GPCR activation assays

To test the new $G\alpha_{i1}$ biosensor in live cell imaging, we employed a well-characterized GPCR known to couple to $G\alpha_{i1}$, the α_2 adrenergic receptor (α_2AR). HeLa cells, shown before to contain the α_2AR endogenously [20], were transfected with the $G\alpha_{i1}$ biosensor. Upon addition of 10μM UK14,304 we observed a robust loss of FRET by measuring the ratio between the YFP and CFP fluorescence of the $G\alpha_{i1}$ biosensor, which was reversed back to baseline by the

addition of 60μM of the α_2AR antagonist Yohimbine (Fig 2A). *Pertussis toxin* (PTX) has been shown to inactivate $G\alpha_i$ signaling in cells via ADP-ribosylation of the $G\alpha_i$ subunit [28], which prevents its interaction with GPCRs. The activation of the $G\alpha_{i1}$ was completely abolished by overnight incubation with PTX, showing that $G\alpha_{i1}$-mTq2 protein fusion is still PTX-sensitive (Fig 2A). To confirm that the sensor can be used to assay $G\alpha_{i1}$ activation of endogenous receptors in primary cells, we repeated this experiment in HUVEC (human umbilical vein endothelial cells). Addition of a well-known stimulant for HUVECs, S1P [29], caused a sustained decrease in FRET ratio of the $G\alpha_{i1}$-sensor (Fig 2B), overnight treatment with PTX completely abolished this response. Next, to investigate how robust the $G\alpha_{i1}$ sensor performs on other GPCR activation assays, we tested a variety of GPCRs shown to couple to $G\alpha_i$. The bradykinin 2B (BK_{2B}) receptor [30], lysophosphatidic acid 2 (LPA_2) receptor [31,32] and muscarinic acetylcholine 3 (M_3) receptor [33,34] were co-transfected with the $G\alpha_{i1}$ biosensor in HeLa cells. Upon stimulation with the relevant agonists, all three receptors showed a sustained decrease in FRET ratio of the $G\alpha_{i1}$ biosensor (Fig 2C). The M_3 receptor also showed a full recovery back to baseline of the FRET ratio after addition of the antagonist atropine. The M_3 receptor is mainly known for its signaling via $G\alpha_q$. Still, previous studies have shown $G\alpha_i$ activation via the M_3 receptor [19,33–36], fitting with with our observations.

In the control conditions, e.g. absence of over-expressed GPCR, we stimulated HeLa cells with the relevant agonist and antagonist, and we observed only a very minor response on the $G\alpha_{i1}$ sensor in the case of LPA stimulation. This is most likely due to the activation of endogenous LPA receptors in HeLa cells [37]. When we co-transfected the β_2 adrenergic receptor (β_2AR), none of the cells showed $G\alpha_{i1}$ activation in response to the agonist and antagonist treatment (Fig 2C). Of note, β_2AR is a classical activator of $G\alpha_s$ but switching to $G\alpha_i$ has been reported under certain conditions [38]. Our results fit with the only study that we are aware of that uses similar tools (BRET based sensors) and similar conditions (over-expressed β_2AR and heterotrimeric G-protein sensors) [19]. Also in that case no activation of $G\alpha_{i1}$ was observed by β_2AR stimulation (and only little activation of $G\alpha_{i2}$ and $G\alpha_{i3}$, which was >10-fold lower than activation by the alpha-2C adrenergic receptor, a strong activator of $G\alpha_i$).

To verify the performance of the $G\alpha_{i2}$ and $G\alpha_{i3}$ biosensors, we transfected HeLa cells with their respective plasmids. Similar to $G\alpha_{i1}$ biosensor experiment in Fig 2A we observed a robust loss of FRET after addition of 10μM UK14,304, and the signal returned to baseline upon addition of 60μM Yohimbine (Fig 2D). Under these experimental conditions we did not observe substantial differences in the activation kinetics or amplitude of the responses between the three different $G\alpha_i$ subunits. Both $G\alpha_{i2}$-mTq2 and $G\alpha_{i3}$-mTq2 are still sensitive to PTX treatment, as shown by the abolishment of the FRET response after overnight incubation with PTX (Fig 2D).

Fast kinetic measurements

In order to look at the sub-second kinetics of $G\alpha_{i1}$ activation in living cells in more detail, HEK293 cells were co-transfected with the $G\alpha_{i1}$-sensor and the α_2AR or adenosine A1 receptor, respectively. Using a fast perfusion system for ligand application, single-cell FRET measurements show a rapid loss in FRET ratio of more than 15% after short-term application of 20μM norepinephrine. After ligand washout, the FRET signal returns to baseline levels. This could be reproduced several times without any apparent loss in signal amplitude (Fig 3A). A similar response was observed for the adenosine A1 receptor after short application of the endogenous ligand adenosine (30μM) (Fig 3B).

These fast FRET measurements can be used to estimate the on-kinetics of $G\alpha_{i1}$ activation with sub second resolution (Fig 3C), as shown by a close-up of the first stimulation in the

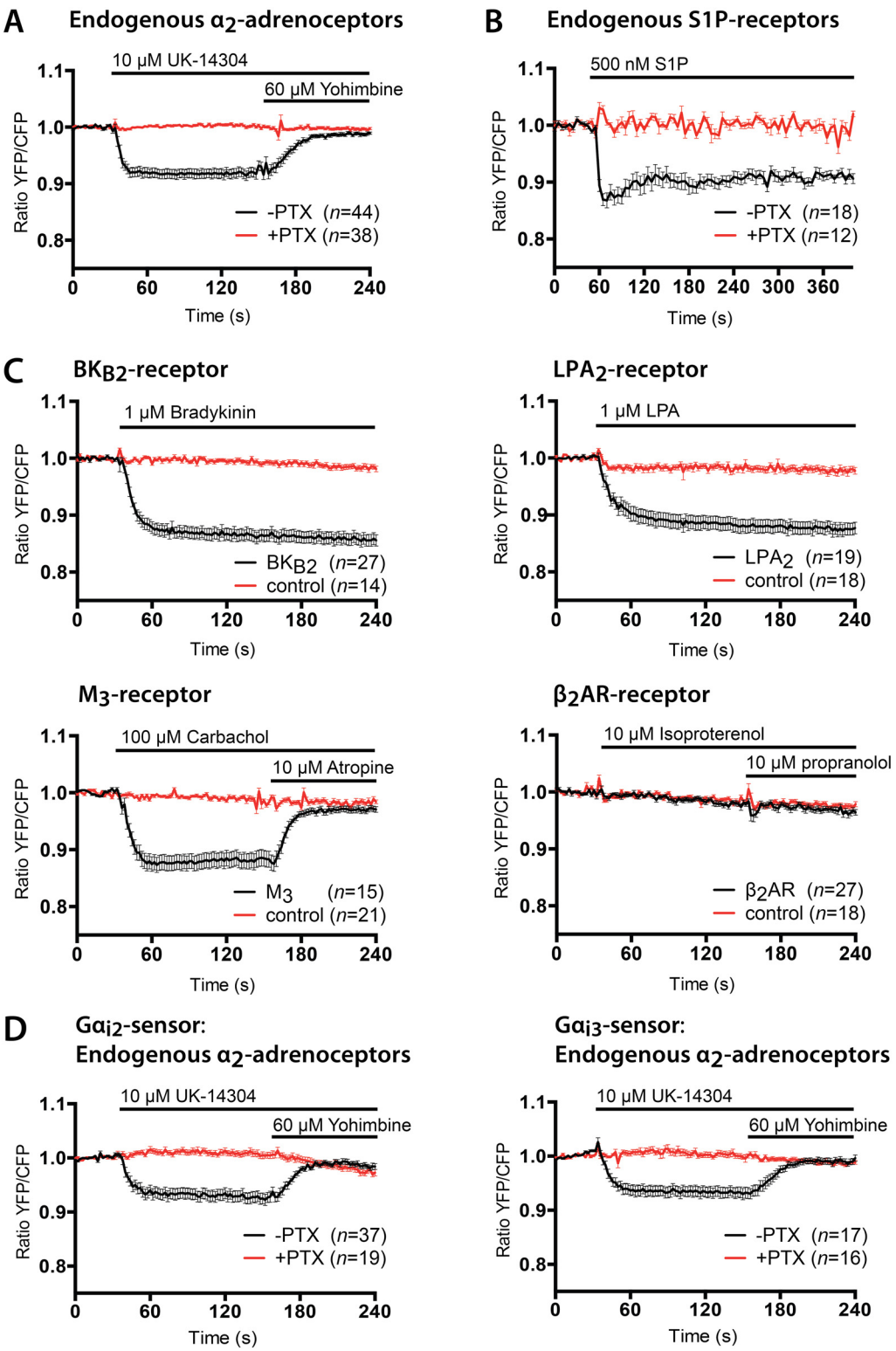

Fig 2. Performance of the Gα$_i$-sensors in single cell GPCR signaling assays. (A) FRET ratio-imaging experiments in HeLa cells transfected with the Gα$_{i1}$-sensor. Rapid loss of FRET, observed by a decreased YFP/CFP ratio, after stimulation of the cells with 10μM UK-14,304, an α_2AR specific agonist, addition of 60μM Yohimbine returns the FRET ratio towards baseline levels. Overnight treatment with (100ng/mL) PTX abolishes the response on the Gα$_{i1}$-sensor in UK-14304 stimulated cells. (B) FRET ratio-imaging experiments in Huvecs transfected with the Gα$_{i1}$-sensor. A sustained loss of FRET is observed after stimulation with 500nM S1P (Sphingosine-1-phosphate). Overnight treatment with (100ng/mL) PTX abolishes the response on the Gα$_{i1}$-sensor in S1P

stimulated cells. (C) FRET ratio-imaging experiments of HeLa cells transfected with the $G\alpha_{i1}$-sensor and BK_{2B} (*top-right*), LPA_2 (*top-left*), M_3 (*bottom-right*) and β_2AR-2A2-mCherry (*bottom-left*) were stimulated with 1μM bradykinin (BK_{2B}), 1μM lysophosphatidic acid (LPA_2), 100μM carbachol and 10μM atropine (M_3) or 10μM isoproterenol and 10μM propranolol (β_2AR). HeLa cells transfected with BK_{2B}, LPA_2 and M_3 receptors show a clear change in YFP/CFP FRET ratio upon addition of their respective agonists, whereas stimulation of the β_2AR does not alter the FRET ratio of the $G\alpha_{i1}$-sensor. In the control conditions, HeLa cells with only the $G\alpha_{i1}$-sensor transfected received identical stimulations. (D) FRET ratio-imaging experiments in HeLa cells transfected with the $G\alpha_{i2}$-sensor or $G\alpha_{i3}$-sensor. Rapid loss of FRET is observed after stimulation of the cells with 10μM UK-14,304, subsequent addition of 60μM Yohimbine returns the FRET ratio towards baseline levels. Overnight treatment with (100ng/mL) *pertussis toxin* (PTX) abolishes the response on the $G\alpha_{i2}$ and $G\alpha_{i3}$ biosensors in UK-14304 stimulated cells. HeLa cells were stimulated with an agonist at t = 32s and an antagonist was added at t = 152s where indicated. Huvec cells were stimulated with S1P at t = 55s. Time traces show the average ratio change of YFP/CFP fluorescence (±s.e.m). Average curves consist of data from at least 3 independent experiments, conducted on different days, with the indicated number of cells (n) per condition.

doi:10.1371/journal.pone.0146789.g002

experiment shown in Fig 3A. The curve was fitted to a one component exponential decay function as previously described [39], resulting in an exponential time constant (τ) of 1160ms.

To assess the precise on-rate kinetics of the $G\alpha_{i1}$-sensor, cells were stimulated with saturating ligand concentrations (100μM norepinephrine or 30μM adenosine). Each individual response was fitted to a one component exponential, this resulted in average τ values for α_2AR of 887ms and for adenosine A1 of 963ms (Fig 3D), corresponding to half-times of 614ms and 668ms respectively. These values are in good agreement with earlier observations for G-protein activation by FRET [21,40,41].

Concluding Remarks

In this manuscript we describe the design, construction and characterization of three new FRET biosensors for the measurement of $G\alpha_{i1}$, $G\alpha_{i2}$, $G\alpha_{i3}$ activation. The new sensors contain a Gα subunit fused to the donor fluorophore, mTurquoise2, and the Gγ subunit fused to cp173Venus, as it was previously shown that this combination for a $G\alpha_q$ FRET sensor provides the largest dynamic range [26]. The three subunits of the heterotrimer ($G\alpha_i$-mTq2, $G\beta_1$ and cpVenus-$G\gamma_2$) were configured on a single plasmid, enabling robust co-expression with a preferred stoichiometry. We show that these sensors are well suited for live cell microscopy and extracting kinetic parameters by single-cell ratiometric FRET imaging. The standardized layout of these FRET biosensors for G-protein activation will improve reliability and reproducibility of experiments within and between laboratories. This is exemplified in this paper by the robust performance of the $G\alpha_{i1}$ sensor in three different laboratories, without optimization of the experimental conditions.

One limitation of energy transfer based biosensors for heterotrimeric G-proteins is that they depend on overexpression of the heterotrimer, which may affect the natural preference of the GPCR for a certain class of heterotrimeric G-proteins. Tagging the endogenous subunits with fluorescent proteins can potentially alleviate this.

The exquisite sensitivity of these sensors enables the robust detection of $G\alpha_i$ activation in primary cells via endogenous GPCRs. Moreover, these biosensors can be used to directly compare the preferential activation patterns of $G\alpha_{i1}$ $G\alpha_{i2}$ and $G\alpha_{i3}$ between different $G\alpha_i$ coupled GPCRs, which can aid the development of therapeutic strategies targeting $G\alpha_i$ signaling pathways [42].

Methods

Construction of fluorescent protein fusions

To insert mTurquoise2-Δ9 (abbreviated here as mTq2) [25] in the $G\alpha_{i1}$, $G\alpha_{i2}$ and $G\alpha_{i3}$ proteins, a version of mTq2 with Age1 restriction sites at its N-terminal and C-terminal was constructed by amplifying mTurquoise2 with forward primer 5′ -ATaccggttctATGGTGAGCAA GGGCG-3′ and reverse primer 5′ -TAaccggtGATCCCGGCGGC-3′ . To introduce an

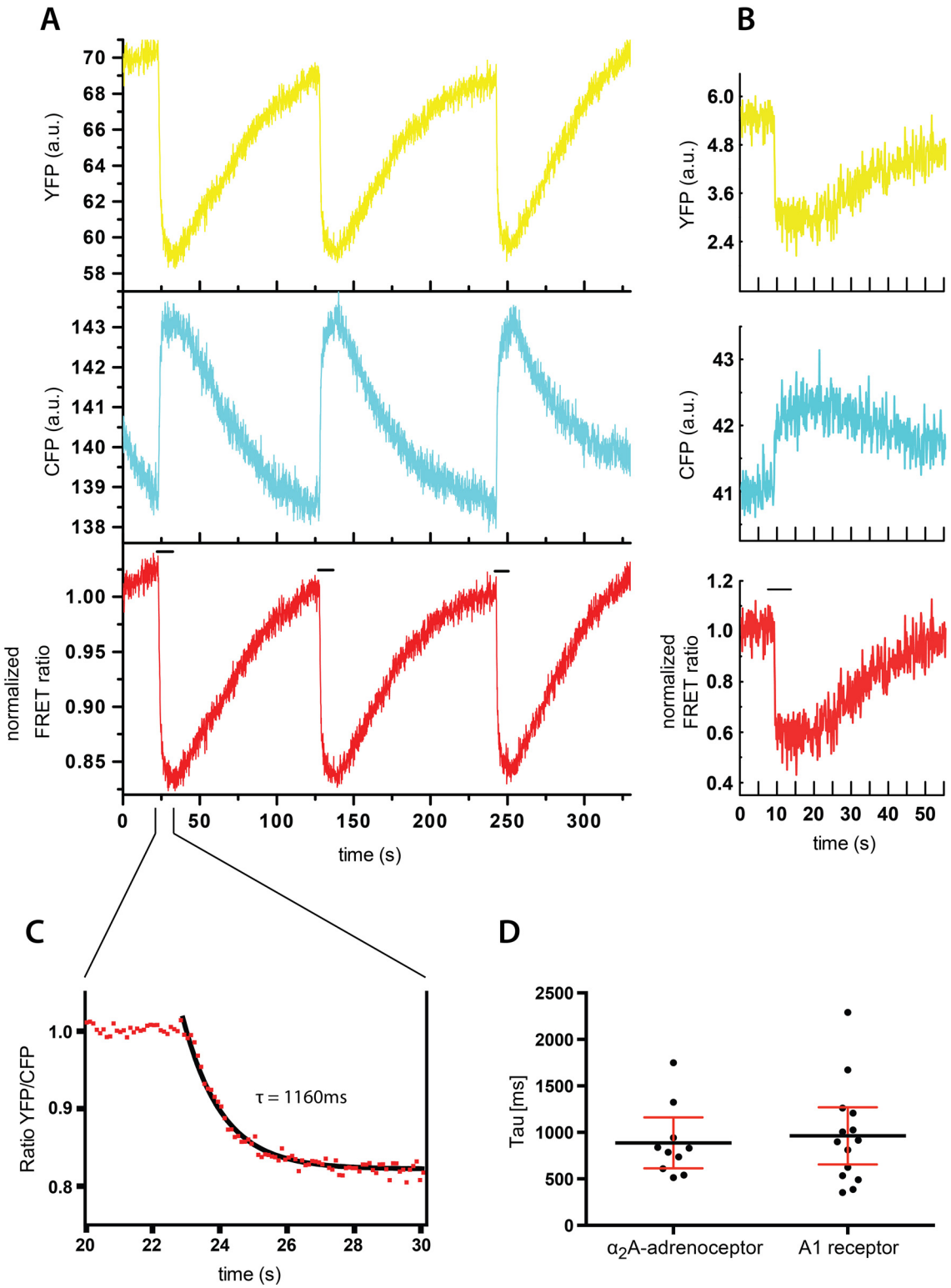

Fig 3. Performance of the Gα$_{i1}$-sensor in kinetic measurements. (A) HEK293 cells transfected with the Gα$_{i1}$-sensor and the α_2AR were repeatedly stimulated with 20μM norepinephrine during intervals that are indicated by short horizontal lines. The presented data is representative for at least six different transfections performed on six experimental days. Top panel: YFP emission, center panel: CFP emission, bottom panel: corrected and normalized FRET ratio. (B) HEK293 cells transfected with the Gα$_{i1}$-sensor and the Adenosine A1-receptor were stimulated with 30μM adenosine, indicated by the short horizontal line. The presented data is representative for at least six different transfections performed on six experimental days. Top panel: YFP emission, center panel: CFP emission, bottom panel: corrected and normalized FRET ratio. (C) A close-up of the on-kinetics of Gα$_{i1}$ activation, showing the normalized

FRET ratio during the first stimulation of the experiment in (A), fitted to a one component exponential decay function with tau = 1160ms and amplitude = 0.18 (R = 0.99). (D) Scatter plot showing the average exponential time constants (tau) of pooled data from (n = 10) individual fits of HEK293 cells transfected with the $G\alpha_{i1}$-sensor and the α_2AR stimulated with 100μM norepinephrine or pooled data (n = 14) from individual fits of the $G\alpha_{i1}$-sensor and the Adenosine A1-receptor stimulated with 30μM adenosine, respectively. Error bars indicate 95% CI.

doi:10.1371/journal.pone.0146789.g003

Age1-site in the $G\alpha_{i1}$-citrine, we performed a whole-vector PCR on template RnGalpha$_{i1}$-Citrine [20] with forward primer 5′ -ATaccggtGAACTCGCCGGCGTCATA-3′ and reverse primer 5′ -ATaccggtCGCGGTCATAAAGCCTTC-3′ . To introduce an Age1-site in the $G\alpha_{i2}$-citrine, we performed a whole-vector PCR on template HsGalpha$_{i2}$-Citrine [20] with forward primer 5′ -ATaccggtGAGGAGCAAGGCGTGCT-3′ and reverse primer 5′ -TAaccggtGGCGGTGCAGGACAGT-3′ . The cDNA containing the coding sequence for HsGalpha$_{i3}$ with an Age1 site was synthesized by Eurofins (www.eurofins.nl). Cutting the mTq2 PCR product and the new $G\alpha_{i1}$, $G\alpha_{i2}$ and $G\alpha_{i3}$ vectors with Age1 and subsequent ligation resulted in RnGalpha$_{i1}$ tagged with mTq2 after position 121, and HsGalpha$_{i2,3}$ tagged with mTq2 after position 114, analogous to a previously reported functionally tagged $G\alpha_{i1,2,3}$ [20].

To construct variant 1.0 of the $G\alpha_{i1}$ sensor, a PCR was performed on the mTq2-$G\alpha_{i1}$ plasmid, with forward primer 5′ -AGGTCTATATAAGCAGAGC-3′ and reverse primer 5′ -TAT ggatccAGCTTAGAAGAGACCACAGTC-3′ to introduce a BamHI site at the C-terminus and an NcoI site at the N-terminus. Next a triple ligation was performed with the PCR product (cut with BamHI and NcoI), a vector containing pGβ_1-T2A-cp173Venus-Gγ_2 [43](cut with BamHI and SacII), and a vector containing pPRIG-IRES [44] (cut with NcoI and SacII). The resulting plasmid, pGβ_1-2A-YFP-Gγ_2-IRES-MATT-$G\alpha_{i1}$-CFP, co-expresses MATT-$G\alpha_{i1}$-mTurquoise2-Δ9 (impaired plasma membrane localization), pGβ_1 and cp173Venus-Gγ_2 (Fig 1B).

To construct variant 2.0 of the $G\alpha_{i1}$-sensor, we performed a mutagenesis PCR with variant 1.0 as template, by amplifying with forward 5'-GAAAAACACGATGATAATATGGGCTGCA CACTGAGC-'3 and 5'-GCTCAGTGTGCAGCCCATATTATCGTGTTTTTC-3'. The resulting plasmid, pGβ_1-2A-cp173Venus-Gγ_2-IRES-$G\alpha_{i1}$-mTurquoise2-Δ9, co-expresses $G\alpha_{i1}$-mTq2 (properly located at the plasma membrane), pGβ_1 and cpVenus-Gγ_2 (Fig 1B).

To create a single plasmid sensor for $G\alpha_{i2}$ and $G\alpha_{i3}$, we performed an overlap extension PCR [45]. $G\alpha_{i2}$-mTq2 was amplified with forward primer '5-acgatgataatATGGGCTG-CACCGTGA-3′ and reverse primer '5 -TATtctagaAGCTCAGAAGAGGCCGCAGT-3′ , and $G\alpha_{i3}$-mTq2 was amplified with forward primer '5-acgatgataatATGGGCTGCACGTTGA-3′ and reverse primer '5 -TATtctagaAGCTTAATAAAGTCCACATTCCT-3′ . Another PCR was performed on the previously described [26] single plasmid $G\alpha_q$-sensor, with forward primer '5- GAAGTTTTTCTGTGCCATCC -3′ and reverse primer '5—GCAGCCCATattat catcgtgtttttcaaag -3′ . Subsequently, the above described PCR product of $G\alpha_{i2}$-mTq2 or $G\alpha_{i3}$-mTq2 were mixed with the PCR product of the $G\alpha_q$-sensor and used as template for a third PCR with forward primer '5- GAAGTTTTTCTGTGCCATCC-3′ and reverse primer '5- TATtctagaAGCTCAGAAGAGGCCGCAGT-3′ , and forward primer '5- GAAGTT TTTCTGTGCCATCC-3′ and reverse primer '5- TATtctagaAGCTTAATAAAGTCCA CATTCCT-3′ , respectively. The resulting PCR products were then ligated into the $G\alpha_q$-sensor backbone with SacII and XbaI, resulting in pGβ-2A- cp173Venus -Gγ_2-IRES-$G\alpha_{i2}$-mTurquoise2-Δ9 and pGβ_1-2A- cp173Venus-Gγ2-IRES-$G\alpha_{i3}$-mTurquoise2-Δ9, respectively. The sequences of the plasmids are available upon request. The plasmids will be distributed through Addgene: http://www.addgene.org/Dorus_Gadella/. RnGα_{i1}-mCitrine and HsGα_{i2}-mCitrine were a kind gift from Scott Gibson [20]. Note that RnGα_{i1} coding sequence differs only one amino acid from human $G\alpha_{i1}$ (S98A). The LPA_2 receptor was obtained from cDNA.org. BK_2R [46], α_2AR [21], M_3R [47] and the A1 receptor [48] were previously described. β_2AR-P2A-mCherry was a kind gift from Anna Pietraszewska (University of Amsterdam).

Cell culture and sample preparation

HeLa cells (American Tissue Culture Collection: Manassas, VA, USA) were cultured at the University of Amsterdam (Amsterdam, the Netherlands) using Dulbecco's Modified Eagle Medium (DMEM) supplied with Glutamax, 10% FBS, Penicillin (100 U/ml) and Streptomycin (100μg/ml). All cell culture media were obtained from Invitrogen (Bleiswijk, NL).

Cells were transfected in a 35 mm dish holding a glass 24 mm Ø #1 coverslip (Menzel- Gläser, Braunschweig, Germany), using 1–2μl Lipofectamine 2000 according to the manufacturer's protocol (Invitrogen), 0.5–1μg plasmid cDNA and 50μl OptiMeM (Life Technologies, Bleiswijk, NL). After overnight incubation at 37°C and 5% CO_2, coverslips were mounted in an Attofluor cell chamber (Invitrogen, Breda, NL) and submerged in microscopy medium (20mM HEPES (PH = 7.4), 137 mM NaCL, 5.4mM KCL, 1.8 mM $CaCL_2$, 0.8mM $MgCl_2$ and 20mM glucose). All live cell microscopy was done at 37°C.

Human umbilical vein endothelial cells (HUVECs) were purchased from Lonza and cultured at Sanquin Blood Supply (Amsterdam, the Netherlands) on FN-coated dishes in EGM-2 medium, supplemented with singlequots (Lonza, Verviers, Belgium). HUVECs were used at passage number 4 or 5. The Neon transfection system (MPK5000, Invitrogen) and a corresponding Neon transfection kit (Invitrogen) were used as transfection method. A single pulse was generated at 1300 Volt for 30ms to microporate HUVECs with 2μg cDNA, cells were subsequently seeded on FN-coated glass coverslips.

For the rapid kinetic measurements of $G\alpha_{i1}$ activation, HEK293 cells were cultivated at the University of Wuerzburg (Wuerzburg, Germany) in Dulbecco's modified Eagle's medium (DMEM) supplemented with 10% fetal calf serum, L-Glutamine (2 mM) (PAN Biotech GmbH, Aidenbach, Germany), Penicillin (100 U/ml), and Streptomycin (100 μg/ml) and kept at 37°C in a 7% CO2 atmosphere. Cells were harvested and seeded onto D-Polylysine-coated 24 mm glass coverslips at ~40% confluency. After three hours cells were transiently transfected with 1.0μg of receptor (α_2AR or adenosine A1) and 3.0 μg $pG\beta_1$-2A-YFP-$G\gamma_2$-IRES-$G\alpha_{i1}$-mTq2 cDNA per 6-well plate using Effectene® transfection reagent (Qiagen), according to the manufacturer's protocol. Growth medium was renewed after 24h and measurements were performed after a total incubation time of 48h. The cells were kept in microscopy medium (140 mM NaCl, 5.4 mM KCl, 2 mM CaCl2, 1 mM MgCl2, 10 mM HEPES, pH 7.3) and permanently superfused with this buffer or buffer supplemented with the appropriate ligand, using a computer-assisted solenoid valve-controlled rapid superfusion device (ValveLink 8.2, Automate Scientific).

Widefield microscopy

Ratiometric FRET measurements in HeLa cells (results presented in Fig 2A, 2C and 2D) were performed using a wide-field fluorescence microscope (Axiovert 200 M; Carl Zeiss GmbH, Germany) at the University of Amsterdam (Amsterdam, the Netherlands), kept at 37°C, equipped with an oil-immersion objective (Plan-Neo- fluor 40×/1.30; Carl Zeiss GmbH) and a xenon arc lamp with monochromator (Cairn Research, Faversham, Kent, UK). Images were recorded with a cooled charged-coupled device camera (Coolsnap HQ, Roper Scientific, Tucson, AZ, USA). Typical exposure times ranged from 75ms to 150ms, and camera binning was set to 4x4. Fluorophores were excited with 420 nm light (slit width 30nm) and reflected onto the sample by a 455DCLP dichroic mirror and CFP emission was detected with a BP470/30 filter, and YFP emission was detected with a BP535/30 filter by rotating the filter wheel. In the co-expression experiments, YFP was excited with 500nm light (slit width 30nm) and reflected onto the sample by a 515DCXR dichroic and emission was detected with a BP535/30 filter. Acquisitions were corrected for background signal and, for FRET ratio imaging, bleedthrough of CFP emission in the YFP channel (55% of the intensity measured in the CFP channel).

For the FRET experiments in HUVECs (results presented in Fig 2B), a Zeiss Observer Z1 microscope was used at Sanquin Blood Supply (Amsterdam, the Netherlands) with a 40x NA 1.3 oil immersion objective and an HXP 120 V excitation light source. CFP was excited through a FRET filter cube (Exciter ET 436/20x, and 455 DCLP dichroic mirror (Chroma, Bellows Falls, Vermont, USA)). The emission was directed to an attached dual camera adaptor (Carl Zeiss GmbH, Germany) controlling a 510 DCSP dichroic mirror (Chroma, Bellows Falls, Vermont, USA). Emission wavelengths between 455–510 nm are directed to an emission filter ET 480/40 (Chroma, Bellows Falls, Vermont, USA) and then captured by a Hamamatsu ORCA-R2 camera. Emission wavelength 510 nm and higher are directed to an ET 540/40m emission filter (Ludl Electronic Products, NY, USA) and then captured by a second Hamamatsu ORCA-R2 camera. Image acquisition was performed using Zeiss-Zen 2011 microscope software. All acquisitions were corrected for background signal. Acquisitions were corrected for background signal and bleedthrough of CFP emission in the YFP channel (62% of the intensity measured in the CFP channel).

For the rapid kinetic measurements of $G\alpha_{i1}$ activation (results presented in Fig 3), imaging was performed on a Zeiss Axiovert 200 inverted microscope at the University of Wuerzburg (Wuerzburg, Germany), equipped with an oil immersion 63x objective lens and a dual-emission photometric system (Till Photonics) as described before [21]. The transfected cells were excited with light from a polychrome IV (Till Photonics). Illumination was set to 40ms out of a total integration time of 100ms. CFP (480 ± 20 nm), YFP (535 ± 15 nm), and FRET ratio (YFP/CFP) signals were recorded simultaneously (beam splitter DCLP 505 nm) upon excitation at 436 ± 10 nm (beam splitter DCLP 460 nm). Fluorescence signals were detected by photodiodes and digitalized using an analogue-digital converter (Digidata 1440A, Axon Instruments). All data were recorded on a PC running Clampex 10.3 software (Axon Instruments). Resulting individual traces were fit to a one component exponential decay function to extract the exponential time constant, tau [39]. The halftime of activation ($t_{1/2}$) is defined as $\tau^*\ln 2$. In dynamic experiments, cells were stimulated with UK14,304 (10μM), Yohimbine (60μM), Bradykinin (1μM), LPA (1μM), Carbachol (100μM), Atropine (10μM), Isoproterenol (10μM), Propranolol (10μM), S1P (500nM), 20μM or 100μM norepinephrine or 30μM adenosine at the indicated time points. ImageJ (National Institute of Health) was used to analyze the raw microscopy images. Further processing of the data was done in Excel (Microsoft Office) and graphs and statistics were conducted using Graphpad version 6.0 for Mac, GraphPad Software, La Jolla California USA, www.graphpad.com.

Confocal microscopy

HeLa cells transfected with the indicated constructs were imaged using a Nikon A1 confocal microscope equipped with a 60x oil immersion objective (Plan Apochromat VC, NA 1.4). The pinhole size was set to 1 Airy unit (<0.8μm).

Samples were sequentially excited with a 457nm and a 514nm laser line, and reflected onto the sample by a 457/514 dichroic mirror. CFP emission was filtered through a BP482/35 emission filter; YFP emission was filtered through a BP540/30 emission filter. To avoid bleedthrough, images were acquired with sequential line scanning modus. All acquisitions were corrected for background signal.

Supporting Information

S1 Data. The compressed file contains all the data that was used in this manuscript.
(ZIP)

Acknowledgments

We thank Eelco Hoogendoorn (University of Amsterdam) and Marten Postma (University of Amsterdam) for assisting in data analysis. We thank Jorrit Broertjes (MsC student at University of Amsterdam) and Dennis Botman (MsC student at University of Amsterdam) for generating $G\alpha_{i1}$-mTurquoise2 and $G\alpha_{i2}$-mTurquoise2, respectively. We thank Merel Adjobo-Hermans, Anna Pietraszewska and Scott Gibson for providing plasmids.

Author Contributions

Conceived and designed the experiments: JvU PLH CH JG TWG. Performed the experiments: JvU ADS BS NRR. Analyzed the data: JvU ADS BS NRR CH JG. Wrote the paper: JvU ADS BS NRR PLH CH TWG JG.

References

1. Suki WN, Abramowitz J, Mattera R, Codina J, Birnbaumer L. The human genome encodes at least three non-allellic G proteins with alpha i-type subunits. FEBS Lett. 1987; 220: 187–192. PMID: 2440724
2. Kimple ME, Neuman JC, Linnemann AK, Casey PJ. Inhibitory G proteins and their receptors: emerging therapeutic targets for obesity and diabetes. Exp Mol Med. 2014; 46: e102. doi: 10.1038/emm.2014.40 PMID: 24946790
3. Wang Y, Li Y, Shi G. The regulating function of heterotrimeric G proteins in the immune system. Arch Immunol Ther Exp (Warsz). 2013; 61: 309–319. doi: 10.1007/s00005-013-0230-5
4. Dorsam RT, Gutkind JS. G-protein-coupled receptors and cancer. Nat Rev Cancer. 2007; 7: 79–94. doi: 10.1038/nrc2069 PMID: 17251915
5. Daaka Y. G proteins in cancer: the prostate cancer paradigm. Sci STKE. 2004; 2004: re2. doi: 10.1126/stke.2162004re2 PMID: 14734786
6. Appleton KM, Bigham KJ, Lindsey CC, Hazard S, Lirjoni J, Parnham S, et al. Development of inhibitors of heterotrimeric Gαi subunits. Bioorg Med Chem. 2014; 22: 3423–3434. doi: 10.1016/j.bmc.2014.04.035 PMID: 24818958
7. Raymond JR, Appleton KM, Pierce JY, Peterson YK. Suppression of GNAI2 message in ovarian cancer. J Ovarian Res. 2014; 7: 6. doi: 10.1186/1757-2215-7-6 PMID: 24423449
8. Garcia A, Kim S, Bhavaraju K, Schoenwaelder SM, Kunapuli SP. Role of phosphoinositide 3-kinase beta in platelet aggregation and thromboxane A2 generation mediated by Gi signalling pathways. Biochem J. 2010; 429: 369–377. doi: 10.1042/BJ20100166 PMID: 20441566
9. la Sala A, Gadina M, Kelsall BL. G(i)-protein-dependent inhibition of IL-12 production is mediated by activation of the phosphatidylinositol 3-kinase-protein 3 kinase B/Akt pathway and JNK. J Immunol. 2005; 175: 2994–2999. PMID: 16116186
10. Kue PF, Daaka Y. Essential role for G proteins in prostate cancer cell growth and signaling. J Urol. 2000; 164: 2162–2167. PMID: 11061948
11. Hur EM, Kim KT. G protein-coupled receptor signalling and cross-talk: achieving rapidity and specificity. Cell Signal. 2002; 14: 397–405. PMID: 11882384
12. Bruce JIE, Straub SV, Yule DI. Crosstalk between cAMP and Ca2+ signaling in non-excitable cells. Cell Calcium. 2003; 34: 431–444. PMID: 14572802
13. Fey D, Croucher DR, Kolch W, Kholodenko BN. Crosstalk and signaling switches in mitogen-activated protein kinase cascades. Front Physiol. 2012; 3: 355. doi: 10.3389/fphys.2012.00355 PMID: 23060802
14. Lohse MJ, Nuber S, Hoffmann C. Fluorescence/bioluminescence resonance energy transfer techniques to study G-protein-coupled receptor activation and signaling. Pharmacol Rev. 2012; 64: 299–336. doi: 10.1124/pr.110.004309 PMID: 22407612
15. van Unen J, Woolard J, Rinken A, Hoffmann C, Hill S, Goedhart J, et al. A Perspective on Studying GPCR Signaling with RET Biosensors in Living Organisms. Mol Pharmacol. 2015; 88(3): 589–595.
16. Gales C, Van Durm JJJ, Schaak S, Pontier S, Percherancier Y, Audet M, et al. Probing the activation-promoted structural rearrangements in preassembled receptor-G protein complexes. Nat Struct Mol Biol. 2006; 13: 778–786. doi: 10.1038/nsmb1134 PMID: 16906158
17. Gales C, Rebois RV, Hogue M, Trieu P, Breit A, Hébert TE, et al. Real-time monitoring of receptor and G-protein interactions in living cells. Nat Methods. 2005; 2: 177–184. doi: 10.1038/nmeth743 PMID: 15782186

18. Ayoub MA, Maurel D, Binet V, Fink M, Prezeau L, Ansanay H, et al. Real-time analysis of agonist-induced activation of protease-activated receptor 1/Galphai1 protein complex measured by bioluminescence resonance energy transfer in living cells. Mol Pharmacol. 2007; 71: 1329–1340. doi: 10.1124/mol.106.030304 PMID: 17267663

19. Saulière A, Bellot M, Paris H, Denis C, Finana F, Hansen JT, et al. Deciphering biased-agonism complexity reveals a new active AT1 receptor entity. Nat Chem Biol. Nature Publishing Group; 2012; 8: 623–631. doi: 10.1038/nchembio.961

20. Gibson SK, Gilman AG. Giα and Gβ subunits both define selectivity of G protein activation by α2-adrenergic receptors. Proc Natl Acad Sci USA. National Academy of Sciences; 2006; 103: 212. doi: 10.1073/pnas.0509763102

21. Bünemann M, Frank M, Lohse MJ. From the Cover: Gi protein activation in intact cells involves subunit rearrangement rather than dissociation. Proc Natl Acad Sci USA. National Academy of Sciences; 2003; 100: 16077. doi: 10.1073/pnas.2536719100

22. Klarenbeek JB, Goedhart J, Hink MA, Gadella TWJ, Jalink K. A mTurquoise-based cAMP sensor for both FLIM and ratiometric read-out has improved dynamic range. PLoS ONE. 2011; 6: e19170. doi: 10.1371/journal.pone.0019170 PMID: 21559477

23. Sparta B, Pargett M, Minguet M, Distor K, Bell G, Albeck JG. Receptor Level Mechanisms Are Required for Epidermal Growth Factor (EGF)-stimulated Extracellular Signal-regulated Kinase (ERK) Activity Pulses. J Biol Chem. 2015; 290: 24784–24792. doi: 10.1074/jbc.M115.662247 PMID: 26304118

24. Hamers D, van Voorst Vader L, Borst JW, Goedhart J. Development of FRET biosensors for mammalian and plant systems. Protoplasma. 2014; 251: 333–347. doi: 10.1007/s00709-013-0590-z PMID: 24337770

25. Goedhart J, Stetten von D, Noirclerc-Savoye M, Lelimousin M, Joosen L, Hink MA, et al. Structure-guided evolution of cyan fluorescent proteins towards a quantum yield of 93%. Nature Communications. 2012; 3: 751. doi: 10.1038/ncomms1738 PMID: 22434194

26. Adjobo-Hermans MJW, Goedhart J, van Weeren L, Nijmeijer S, Manders EMM, Offermanns S, et al. Real-time visualization of heterotrimeric G protein Gq activation in living cells. BMC Biol. 2011; 9: 32. doi: 10.1186/1741-7007-9-32 PMID: 21619590

27. Goedhart J, van Weeren L, Adjobo-Hermans MJW, Elzenaar I, Hink MA, Gadella TWJ. Quantitative Co-Expression of Proteins at the Single Cell Level–Application to a Multimeric FRET Sensor. Delprato AM, editor. PLoS ONE. 2011; 6: e27321. PMID: 22114669

28. Burns DL. Subunit structure and enzymic activity of pertussis toxin. Microbiol Sci. 1988; 5: 285–287. PMID: 2908558

29. Wang F, Van Brocklyn JR, Hobson JP, Movafagh S, Zukowska-Grojec Z, Milstien S, et al. Sphingosine 1-phosphate stimulates cell migration through a G(i)-coupled cell surface receptor. Potential involvement in angiogenesis. J Biol Chem. 1999; 274: 35343–35350. PMID: 10585401

30. Liao JK, Homcy CJ. The G proteins of the G alpha i and G alpha q family couple the bradykinin receptor to the release of endothelium-derived relaxing factor. J Clin Invest. 1993; 92: 2168–2172. doi: 10.1172/JCI116818 PMID: 8227332

31. van Corven EJ, Groenink A, Jalink K, Eichholtz T, Moolenaar WH. Lysophosphatidate-induced cell proliferation: identification and dissection of signaling pathways mediated by G proteins. Cell. 1989; 59: 45–54. PMID: 2551506

32. An S, Bleu T, Hallmark OG, Goetzl EJ. Characterization of a novel subtype of human G protein-coupled receptor for lysophosphatidic acid. J Biol Chem. 1998; 273: 7906–7910. PMID: 9525886

33. Offermanns S, Wieland T, Homann D, Sandmann J, Bombien E, Spicher K, et al. Transfected muscarinic acetylcholine receptors selectively couple to Gi-type G proteins and Gq/11. Mol Pharmacol. 1994; 45: 890–898. PMID: 8190105

34. Akam EC, Challiss RA, Nahorski SR. G(q/11) and G(i/o) activation profiles in CHO cells expressing human muscarinic acetylcholine receptors: dependence on agonist as well as receptor-subtype. Br J Pharmacol. 2001; 132: 950–958. doi: 10.1038/sj.bjp.0703892 PMID: 11181437

35. Hornigold DC, Mistry R, Raymond PD, Blank JL, Challiss RAJ. Evidence for cross-talk between M2 and M3 muscarinic acetylcholine receptors in the regulation of second messenger and extracellular signal-regulated kinase signalling pathways in Chinese hamster ovary cells. Br J Pharmacol. 2003; 138: 1340–1350. doi: 10.1038/sj.bjp.0705178 PMID: 12711635

36. Blaukat A, Barac A, Cross MJ, Offermanns S, Dikic I. G protein-coupled receptor-mediated mitogen-activated protein kinase activation through cooperation of Galpha(q) and Galpha(i) signals. Molecular and Cellular Biology. 2000; 20: 6837–6848. PMID: 10958680

37. Jongsma M, Matas-Rico E, Rzadkowski A, Jalink K, Moolenaar WH. LPA is a chemorepellent for B16 melanoma cells: action through the cAMP-elevating LPA5 receptor. PLoS ONE. 2011; 6: e29260. doi: 10.1371/journal.pone.0029260 PMID: 22195035

38. Hill SJ, Baker JG. The ups and downs of Gs- to Gi-protein switching. Br J Pharmacol. 2003; 138: 1188–1189. doi: 10.1038/sj.bjp.0705192 PMID: 12711616

39. Hoffmann C, Gaietta G, Bünemann M, Adams SR, Oberdorff-Maass S, Behr B, et al. A FlAsH-based FRET approach to determine G protein-coupled receptor activation in living cells. Nat Methods. 2005; 2: 171–176. doi: 10.1038/nmeth742 PMID: 15782185

40. Hein P, Rochais F, Hoffmann C, Dorsch S, Nikolaev VO, Engelhardt S, et al. GS Activation Is Time-limiting in Initiating Receptor-mediated Signaling. Journal of Biological Chemistry. 2006; 281: 33345–33351. doi: 10.1074/jbc.M606713200 PMID: 16963443

41. Hoffmann C, Nuber S, Zabel U, Ziegler N, Winkler C, Hein P, et al. Comparison of the Activation Kinetics of the M3-ACh-receptor and a Constitutively Active Mutant Receptor in Living Cells. Mol Pharmacol. 2012; 82(2): 236–245 doi: 10.1124/mol.112.077578 PMID: 22564786

42. Devanathan V, Hagedorn I, Köhler D, Pexa K, Cherpokova D, Kraft P, et al. Platelet Gi protein Gαi2 is an essential mediator of thrombo-inflammatory organ damage in mice. Proc Natl Acad Sci USA. 2015; 112: 6491–6496. doi: 10.1073/pnas.1505887112 PMID: 25944935

43. Nagai T, Yamada S, Tominaga T, Ichikawa M, Miyawaki A. Expanded dynamic range of fluorescent indicators for Ca(2+) by circularly permuted yellow fluorescent proteins. Proc Natl Acad Sci USA. 2004; 101: 10554–10559. doi: 10.1073/pnas.0400417101 PMID: 15247428

44. Martin P, Albagli O, Poggi MC, Boulukos KE, Pognonec P. Development of a new bicistronic retroviral vector with strong IRES activity. BMC Biotechnol. 2006; 6: 4. doi: 10.1186/1472-6750-6-4 PMID: 16409632

45. Heckman KL, Pease LR. Gene splicing and mutagenesis by PCR-driven overlap extension. Nat Protoc. 2007; 2: 924–932. doi: 10.1038/nprot.2007.132 PMID: 17446874

46. Adjobo-Hermans MJW, Goedhart J, Gadella TWJ. Regulation of PLCbeta1a membrane anchoring by its substrate phosphatidylinositol (4,5)-bisphosphate. Journal of Cell Science. 2008; 121: 3770–3777. doi: 10.1242/jcs.029785 PMID: 18957514

47. Ziegler N, Bätz J, Zabel U, Lohse MJ, Hoffmann C. FRET-based sensors for the human M1-, M3-, and M5-acetylcholine receptors. Bioorg Med Chem. 2011; 19: 1048–1054. doi: 10.1016/j.bmc.2010.07.060 PMID: 20716489

48. Klotz KN, Hessling J, Hegler J, Owman C, Kull B, Fredholm BB, et al. Comparative pharmacology of human adenosine receptor subtypes—characterization of stably transfected receptors in CHO cells. Naunyn Schmiedebergs Arch Pharmacol. 1998; 357: 1–9. PMID: 9459566